Cancer Immunol Immunother (2012) 61:409–424
DOI 10.1007/s00262-011-1112-5

ORIGINAL ARTICLE

Inclusive estimation of complex antigen presentation functions of monocyte-derived dendritic cells differentiated under normoxia and hypoxia conditions

Toshitatsu Ogino · Hideya Onishi · Hiroyuki Suzuki · Takashi Morisaki · Masao Tanaka · Mitsuo Katano

Received: 10 May 2011 / Accepted: 6 September 2011 / Published online: 20 September 2011

Abstract Dendritic cells (DCs) generated from monocytes under 20% O_2 are now used as therapeutic tools for cancer patients. However, the O_2 concentration is between 3 and 0.5% in most tissues. We evaluated these complicated functions of DCs under oxygen tensions mimicking in vivo situations. Immature DCs (imDCs) were generated from monocytes using IL-4 and GM-CSF under normoxia (20% O_2; N-imDCs) or hypoxia (1% O_2; H-imDCs). Mature DCs (mDCs) were induced with LPS. DCs were further exposed to normoxia (N/N-DCs) or hypoxia (N/H-DCs and H/H-DCs) conditions. Using a 2-D culture system, H-DCs were smaller in size than N-DCs, and H/H-DCs exhibited higher allo-T cell stimulation ability than N/N-DCs and N/H-DCs. On the other hand, motility and phagocytic ability of H/H-DCs were significantly lower than those of N/H-DCs and N/N-DCs. In a 3-D culture system, however, maturation of H/H-imDCs and N/H-imDCs was suppressed compared with N/N-imDCs as a result of their decreased motility and phagocytosis. Interestingly, silencing of *HIF-1α* by RNA interference decreased CD83 expression without affecting any antigen presentation abilities except for the ability to stimulate the allo-T cell population. Our data could help our understanding of DCs, especially therapeutic DCs, in vivo.

Keywords Hypoxia · Dendritic cells · Complex antigen presentation functions · Immunotherapy

Abbreviations

MFI	Mean fluorescence intensity
VEGF	Vascular endothelial cell growth factor
HIF-1α	Hypoxia inducible factor-1α
Treg	Regulatory T cell
CA9	Carbonic anhydrase IX
3-D	Three-dimensional

Introduction

Dendritic cells (DCs) originate from $CD34^+$ bone marrow progenitors [1], and under certain conditions, monocytes can also differentiate into DCs [2]. It has been reported that oxygen tension is 5.3% in mixed venous blood, typically 3.3–7.9% O_2 in well-vascularized organs, and 0.5% in the lymphoid organs [3]. In tumor tissues, it has been suggested to be lower than 1.3% [4]. Thus, DCs move between 8% O_2 and 0.5% O_2 conditions. On the other hand, therapeutic monocyte-derived DCs are usually generated from peripheral blood monocytes using GM-CSF and IL-4 under 20% O_2 conditions (termed normoxia) in vitro, and their antigen presentation abilities are also estimated under normoxia [5–7]. However, these therapeutic DCs are injected subcutaneously and the injected DCs move to regional lymph nodes for antigen presentation to suitable CD4 and CD8 T cells [8–10]. Thus, therapeutic DCs move

T. Ogino · H. Onishi · H. Suzuki · M. Katano (✉)
Department of Cancer Therapy and Research, Graduate School of Medical Sciences, Kyushu University, 3-1-1 Maidashi, Higashi-ku, Fukuoka 812-8582, Japan
e-mail: mkatano@tumor.med.kyushu-u.ac.jp

T. Morisaki
Fukuoka Cancer General Clinic, Fukuoka, Japan

M. Tanaka
Department of Surgery and Oncology, Kyushu University, Fukuoka, Japan

between 20% O_2 and 0.5% O_2 conditions. DCs are exposed to various oxygen tensions in vivo.

We also know that oxygen tension, especially hypoxia below 1% O_2 conditions, affects biological functions of various types of cells such as tumor cells and leukocytes [11, 12]. For example, it has been shown that hypoxia affects the expression of antigen presentation–related molecules and migratory ability of monocytes or DCs [13–15]. It is still controversial, however, how hypoxia affects these DC functions. In addition, antigen presentation of DCs to T cells is very complex. To induce effective CTLs in the lymphoid organs, DCs must capture tumor antigens at tumor sites, process the antigen, invade into the lymph vessels, migrate to lymph nodes, present the antigen to suitable T cells, and secrete suitable cytokines such as IL-12 [5, 6].

In this study, we tried, for the first time, to evaluate inclusively these complex antigen presentation–related functions under oxygen tensions mimicking in vivo situations [16, 17]. Our data may help our understanding of DCs, especially therapeutic DCs, in vivo.

Materials and methods

Cells and culture conditions

PBMCs were collected from the heparinized peripheral blood of healthy volunteers by HISTOPAQUE-1077 (St. Louis, MO, USA) density gradient centrifugation. $CD14^+$ monocytes were affinity-purified using the MACS^{TM} $CD14^+$ isolation kit (Miltenyi Biotec, Bergisch Gladbach, Germany) following the manufacturer's instruction. The purity of the monocytes was >95% as determined by FACS analysis. DCs were generated from monocytes by incubation for 5 days at 5×10^5 cells/ml in RPMI 1640 medium (Nacalai Tesque, Kyoto, Japan) supplemented with 10% FBS (Life Technologies, Grand Island, NY, USA) containing GM-CSF (100 ng/ml, North China Pharmaceutical Group Corporation-Gene Tech, China) and IL-4 (50 ng/ml, Osteogenetics, Wuerzburg, Germany). To induce maturation, 1 μg/ml LPS from *Escherichia coli* 011: B4 (Sigma, St Louise, Missouri) for 2 days was added. In the induction of DC differentiation, we did not change medium during the culture period. LPS containing medium were treated under hypoxia in advance for 12 h before use.

N/N-DCs: DCs differentiated under normoxia (21% O_2, 5% CO_2, and 74% N_2) (N-DCs) were exposed to normoxia. N/H-DCs: DCs differentiated under normoxia (N-DCs) were exposed to hypoxia. H/H-DCs: DCs differentiated under hypoxia (H-DCs) were exposed to hypoxia. Hypoxia treatment (1% O_2, 5% CO_2, and 94% N_2) was performed by placing cells in the InVivo2 400 hypoxia workstation (SANYO, Tokyo, Japan) maintained at 1% O_2 and 37°C.

Immunoblot analysis

Whole-cell lysates were extracted from the cultured cells using M-PER (Mammalian Protein Extraction) Reagents (Pierce Biotechnology, Rockford, IL, USA) according to the manufacturer's instructions. The protein concentration was determined with a Bio-Rad Protein Assay (Bio-Rad, Hercules, CA, USA). The whole-cell extract (30 μg) was separated by SDS–PAGE and transferred to nitrocellulose membranes (Protran, Dassel, Germany). The blots were then incubated with an anti-HIF-1α (Cell Signaling Technology; Danvers, MA, USA; 1:100) overnight at 4°C. The blots were then incubated in HRP-linked secondary antibody (Amersham Biosciences, Piscataway, NJ, USA) at room temperature for 1 h. Immunocomplexes were detected with the ECL plus Western Blotting Detection System (Amersham Biosciences) and visualized with a Molecular Imager FX (Bio-Rad).

FACS analysis

DCs were stained with fluorescence-labeled anti-CD14, anti-CD11c, anti-CD80, anti-CD83, anti-CD86, anti-HLA-ABC, anti-HLA-DR, anti-CCR5, and anti-CCR7 (BD Biosciences, San Jose, CA, USA). Two-color flow cytometry was performed using a FACSCalibur^{TM} (Becton–Dickinson Immunocytometry Systems, San Jose, CA, USA), and data were analyzed with CELLQuest software. Expression levels were determined as mean fluorescence intensity (MFI).

Real-time RT-PCR

Total RNA was extracted using a High Pure RNA Isolation kit (Roche, Mannheim, Germany) and quantified by spectrophotometry (Ultrospec 2100 Pro; Amersham Pharmacia Biotech, Cambridge, UK). For real-time RT-PCR, 0.5 μg of RNA was treated with DNase and was reverse transcribed to cDNA with the Quantitect Reverse Transcription kit (Qiagen, Valencia, CA, USA) according to the manufacturer's protocol. Reactions were run with iQ SYBR Green Supermix (Bio-Rad, Hercules, CA, USA), on a DNA Engine Option 2 System (MJ Research, Waltham, MA, USA). All primer sets amplified fragments <200-bp long. The primer sequences used were as follows: *matrix metalloproteinase9* (*MMP9*), forward, 5′-TGGGCTACGT GACCTATGACAT-3′, reverse, 5′-GCCCAGCCCACCTC CACTCCTC-3′; *matrix metalloproteinase2* (*MMP2*), forward, 5′-ACCCCCAGTCCTATCTGCC-3′, reverse, 5′-TG GGAACGCCTGACTTCAG-3′; *HIF-1α*, forward, 5′-GAA

GTGTACCCTAACTAGCCGAGG-3′, reverse, 5′-TTTCT TATACCCACACTGAGGTTGG-3′; and *β-actin*, forward, 5′-TTGCCGACAGGATGCAGAAGGA-3′, reverse, 5′-AG GTGGACAGCGAGGCCAGGAT-3′. The amount of each target gene in a given sample was normalized to the level of *β-actin*.

Clinical samples and fluorescence immunohistochemistry

Surgical specimens were obtained from patients with pancreatic ductal adenocarcinoma, all of whom underwent resection at the Department of Surgery and Oncology, Kyushu University (Fukuoka, Japan). Informed consent was obtained from all patients. Samples were fixed in 10% formalin and embedded in paraffin. Slides were dewaxed, rehydrated, washed, and subjected to microwave antigen retrieval in a citrate buffer (pH 6.0). For immunofluorescence double staining, sections were double-stained with rabbit anti-CA9 (Carbonic Anhydrase IX Antibody; 1:100; Novus Biologicals, Littleton, CO, USA) and mouse monoclonal anti-fascin (clone 55 k-2; 1:100; Dako Cytomation, Carpenteria, CA, USA). The bound antibodies were visualized using goat anti-rabbit IgG (H+L) Alexa 488 (Invitrogen, Carlsbad, CA, USA) and goat anti-mouse (H+L) Alexa 568 (Invitrogen). The stained sections were photographed with a digital camera attached to a Zeiss Axio Imager A1 microscope (Carl Zeiss, Oberknochen, Germany).

Allogeneic T-cell proliferation assay

$CD3^+$ T cells were selected from PBMCs using the Dynabeads FlowComp Human CD3 kit (Invitrogen). $CD3^+$ lymphocytes were labeled with 2 μM CFSE (Molecular Probes, Leiden, Netherlands) in PBS at 37°C for 10 min. DCs were induced in the presence of IL-4 and GM-CSF under normoxia (N-DCs) or hypoxia (H-DCs). Then T cells were co-cultured with allogeneic N-DCs at 1:5, 1:10, or 1:20 DCs/T cells ratio for 5 days under normoxia (N/N-DCs/T cells) or hypoxia (N/H-DCs/T cells). In addition, T cells were co-cultured with allogeneic H-DCs under hypoxia (H/H-DCs). Lymphocyte proliferation was assessed by the CFSE dilution method. In T-cell proliferation assay, conditioned medium were treated under hypoxia in advance for 12 h before use.

Evaluation of phagocytosis

DCs were cultured in RPMI 1640 medium supplemented with 10% FBS with either FITC-dextran (Sigma), which were first coated with serum (opsonization), or necrotic cells labeled with PKH26 (Sigma) for 1 or 2 h, respectively, at 37°C or 4°C in normoxia or hypoxia. Necrotic cells were labeled with PKH26 according to the manufacturer's protocol. The DCs were washed, and the fluorescence intensity was measured by FACS analysis. In phagocytosis assay, conditioned medium were treated under hypoxia in advance for 12 h before use.

Matrigel invasion assay

The invasiveness of DCs was assessed based on the invasion of cells through Matrigel-coated transwell inserts. In brief, the upper surface of a filter (pore size, 8.0 μm; BD Biosciences, Heidelberg, Germany) was coated with basement membrane Matrigel (BD Biosciences). DCs were added to the upper chamber and incubated for 16 h subsequently under normoxia or hypoxia in the presence (chemoinvasion assay) or absence (invasion assay) of 100 ng/ml recombinant human RANTES (CCL5) and 6Ckine (CCL21) (R&D Systems) in culture media in the lower chambers. After incubation, the filter was fixed and stained with Diff-Quik reagent (International Reagents, Kobe, Japan). Cells that had migrated from the upper to the lower side of the filter were counted under a light microscope (BX50; Olympus, Tokyo, Japan) at a magnification of ×100. In motility assay, conditioned medium were treated under hypoxia in advance for 12 h before use. The random migration ability of DCs was assessed in the same way as described above, but chilled type 1 collagen (Kokencellgen I-AC: 0.3%) (Funakoshi, Tokyo, Japan)–coated transwell inserts were used.

Chemotaxis assay

To the lower chamber, 100 ng/ml of recombinant human RANTES (CCL5) and 6Ckine (CCL21) or control conditioned medium was added, and the upper surface of a filter (pore size, 8.0 μm) was placed into the wells. The upper surface of a filter was coated with chilled type 1 collagen. A total of 50 μl of cell suspensions (10^6/ml) were seeded in the upper chamber, and the chamber was incubated at 37°C for 3 h under normoxia or hypoxia. At the end of this period, cells that had migrated from the upper to the lower side of the filter were counted under a light microscope at a magnification of ×100.

3-D two-layer collagen gel culture model

We used our developed 3-D two-layer collagen gel culture model to estimate inclusively complex antigen presentation functions of DCs in vivo [16]. Briefly, DCs were used at 4×10^5 cells per assay and suspended in 20-μl RPMI containing 10% FBS under normoxia or hypoxia. DCs were mixed with an equal volume of chilled type 1

collagen to a final concentration of 0.15%. The mixture was then transferred to 96-well plates (Nalge Nunc International, Rochester, NY) at 40 μl/well. Before the mixture was allowed to polymerize, a mixture of 20 μl RPMI with 10% FBS containing 4×10^5 necrotic cells mixed with an equal volume of chilled type 1 collagen was layered onto the DCs mixture. The two layers of mixture were then allowed to polymerize for approximately 1 h at 37°C. After polymerization, 200 μl RPMI with 10% FBS was added to each well. These 3-D two-layer cultures were then incubated at 37°C in a humidified atmosphere of 5% CO_2 under normoxia or hypoxia. Liquid culture medium was changed every day and stored at −80°C for later analysis. DCs were harvested from the collagen matrix by digestion with 7,500 U/ml collagenase (Wako, Osaka, Japan) for 5 min. Cells were washed twice with PBS (Wako) and resuspended in RPMI for further study.

Capture of necrotic cells by DCs in 3-D two-layer collagen culture model

DCs and fluorescently labeled necrotic cells were embedded separately into collagen under normoxia or hypoxia. The DCs were harvested from the collagen matrix, and the fluorescence intensity was measured by FACS analysis.

Enzyme-linked immunosorbent assay (ELISA)

The concentration of hVEGF and hIL-12, biologically active form, levels in DCs supernatants was measured using specific Duo-Set kits purchased from R&D Systems (Minneapolis, MN) in accordance with the manufacturer's instructions.

RNA interference

The siRNA for *MMP9* (ON-TARGET*plus* SMART pool, L-005970), *HIF-1α* (ON-TARGET*plus* SMART pool, L-004018), and negative control siRNA (ONTARGET*plus* siCONTROL non-targeting pool, D-001810) were purchased from Dharmacon RNA Technologies (Chicago, IL, USA). Monocytes seeded in six-well plates at 1×10^6 cells/ml were transfected with 100 nM siRNA using Lipofectamine RNAiMAX Reagent (Invitrogen) for 48 h according to the manufacturer's instructions. DCs were generated from monocytes after transfection.

Statistical analysis

Data were expressed as the mean ± SD. Student's t test was used for statistical analysis. All results with a $P \leq 0.05$ were considered statistically significant.

Fig. 1 DCs differentiated under hypoxia are small in size and express higher antigen presentation–related molecules. **a** Monocytes were cultured for 5 days with IL-4 and GM-CSF and induced for further maturation by treatment with LPS for 48 h under normoxia or hypoxia (N-DCs and H-DCs, respectively). **b** H-DCs express inducible HIF-1α in response to hypoxia. Whole protein extracts were analyzed by Western blot. **c** FACS analysis showed hypoxia significantly changes forward and side scatter properties of DCs (*left panel*). Cell count values represent the mean size of DCs in the range from 12 to 20 μm. H-DCs were smaller than N-DCs (*right panel*). The average of five independent experiments is shown. *Bars* show the means plus SD. $^{**}P < 0.01$ versus N-DCs is shown. **d** mRNA expression was measured by real-time RT-PCR. Expression of MMP2 mRNA was slightly, but not significantly, enhanced in H-imDCs (*left panel*). mRNA expression of MMP9 in HimDCs was decreased (*right panel*). **e** VEGF and IL-12 secretion by DCs under normoxia or hypoxia was measured by ELISA. The production of VEGF was much higher in H-DCs than N-DCs (*left panel*). IL-12 production of H-mDCs was lower than that of N-mDCs (*right panel*). The average of three independent experiments is shown. *Bars* show the means plus SD. $^{**}P < 0.01$ versus N-DCs is shown

Results

DCs differentiated under hypoxia are small in size and express higher antigen presentation–related molecules

DCs, differentiated under normoxia and hypoxia, were tentatively termed N-DCs and H-DCs, respectively (Fig. 1a). To support hypoxia in the present study, HIF-1α expression by DCs was first examined by Western blot analysis. As expected, HIF-1α expression of H-DCs was increased compared with N-DCs (Fig. 1b). The number of H-DCs was similar to that of N-DCs (*data not shown*), but interestingly, the H-DCs were smaller than N-DCs (Fig. 1c). We next examined the expression of antigen presentation–related molecules on DCs by FACS analysis (Table 1). In imDCs, only HLA-DR expression of the H-imDCs was significantly higher than that of N-imDCs. In mDCs, expressions of CD80, CD86, and CD83 in H-mDCs were higher than those in N-mDCs. In addition, the MFI of CD80 and HLA-DR expression in H-mDCs was higher than that in N-mDCs. These results indicate that H-DCs may have higher antigen presentation ability than N-DCs. Next, we examined the effect of hypoxia on the invasion ability. There were no significant differences in *MMP2* mRNA expression between H-DCs and N-DCs (Fig. 1d, *left*). However, *MMP9* mRNA expression of H-DCs was lower than that of N-DCs (Fig. 1d, *right*). Finally, the production of VEGF and IL-12, which are concerned with antigen presentation, was compared. The production of VEGF was much higher in H-DCs than N-DCs (Fig. 1e, *left*). On the other hand, IL-12 production of H-mDCs was lower than that of N-mDCs (Fig. 1e, *right*).

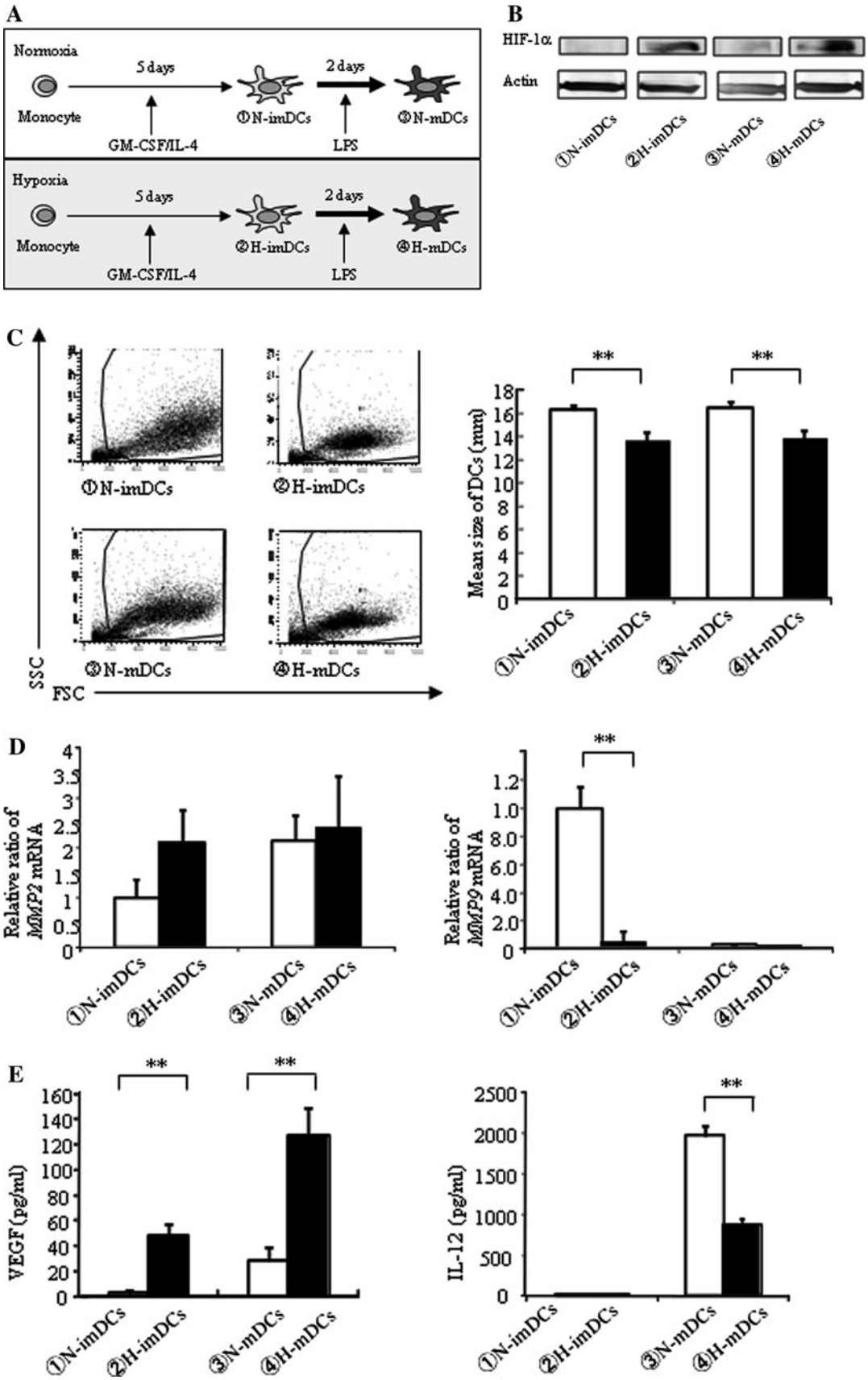
A
Normoxia
5 days
2 days
Monocyte
①N-imDCs
③N-mDCs
GM-CSF/IL-4
LPS
Hypoxia
5 days
2 days
Monocyte
②H-imDCs
④H-mDCs
GM-CSF/IL-4
LPS
B
HIF-1α
Actin
①N-imDCs
②H-imDCs
③N-mDCs
④H-mDCs
C
①N-imDCs
②H-imDCs
③N-mDCs
④H-mDCs
SSC
FSC
**
**
Mean size of DCs (mm)
①N-imDCs
②H-imDCs
③N-mDCs
④H-mDCs
D
Relative ratio of MMP2 mRNA
①N-imDCs
②H-imDCs
③N-mDCs
④H-mDCs
**
Relative ratio of MMP9 mRNA
①N-imDCs
②H-imDCs
③N-mDCs
④H-mDCs
E
**
**
VEGF (pg/ml)
①N-imDCs
②H-imDCs
③N-mDCs
④H-mDCs
**
IL-12 (pg/ml)
①N-imDCs
②H-imDCs
③N-mDCs
④H-mDCs

Table 1 Expression of antigen presentation–related molecules on DCs under normoxia and hypoxia

	①N-imDCs	②H-imDCs	③N-mDCs	④H-mDCs
CD80	16.70 ± 4.29	13.70 ± 10.66	82.55 ± 5.23	91.77 ± 11.82*
	(11.31 ± 3.45)	(6.99 ± 1.68)	(63.47 ± 8.01)	(105.31 ± 20.27)**
CD86	52.63 ± 19.38	30.82 ± 5.94	95.17 ± 2.35	98.59 ± 1.28
	(97.07 ± 40.03)	(76.5 ± 32.71)	(1,047.30 ± 165.86)	(1,551.78 ± 271.92)**
HLA-ABC	97.47 ± 2.18	98.76 ± 1.26	97.77 ± 2.12	98.84 ± 1.18
	(142.41 ± 40.1)	(169.66 ± 53.27)	(778.38 ± 104.51)	(784.78 ± 165.36)
HLA-DR	57.95 ± 13.24	72.16 ± 4.29*	90.37 ± 4.35	93.04 ± 2.28
	(43.87 ± 7.94)	(75.58 ± 15.72)**	(156.79 ± 20.63)	(193.04 ± 37.61)**
CD83	4.36 ± 1.26	4.96 ± 1.53	76.09 ± 3.81	86.85 ± 5.61*
	(6.58 ± 0.55)	(5.07 ± 1.17)	(31.53 ± 7.74)	(46.85 ± 9.51)

Expression of CD80, CD86, CD83, HLA-ABC, and HLA-DR was analyzed by FACS analysis. DCs, differentiated under normoxia and hypoxia, were tentatively termed N-DCs and H-DCs, respectively

Data are presented as the percentage of positive cells of five independent donors (MFI of each marker), mean ± SD

* $P < 0.05$ (① versus ②, ③ versus ④: percentage of positive cells)

** $P < 0.05$ (① versus ②, ③ versus ④: MFI)

DCs differentiated under hypoxia exhibit higher allo-T cell proliferating ability

Monocytes differentiate DCs under hypoxia into tissues with 3–8% O_2 in vivo, and differentiated DCs move into tumor tissues with 1–1.5% O_2 (Fig. 2a; in vivo model). On the other hand, DCs generated from monocytes under 20% O_2 conditions in vitro are injected into subcutaneous tissue with 3–8% O_2 conditions and move to lymph nodes below 0.5% O_2 (Fig. 2a; therapeutic model). To mimic these situations, experiments were performed under normoxia and hypoxia. When N-DCs were exposed to normoxia or hypoxia, these DCs were named N/N-DCs or N/H-DCs, respectively. Similarly, when H-DCs were exposed to hypoxia, DCs were named H/H-DCs (Fig. 2a). To support our in vivo-mimicking model, we examined the expression of both CA9, a target molecule of HIF-1α, and fascin, a marker of DCs, on DCs found in tumor tissues and lymph nodes. As expected, many tumor cells and lymphocytes expressed CA9 (Fig. 2b, *left*) and there is a possibility that small infiltrating fascin-positive mononuclear cells were DCs (Fig. 2b). Table 1 shows that H-mDCs exhibit higher expression of antigen presentation–related molecules than N-mDCs. We therefore examined whether H-mDCs can stimulate allo-T cell proliferation rather than N-mDCs. For this study, allogeneic T cells were first labeled with CFSE and then CSFE-labeled T cells were co-stimulated with N-mDCs under normoxia (N/N-mDCs) or hypoxia (N/H-mDCs) or with H-mDCs under hypoxia (H/H-mDCs) (Fig. 2c). The rate of proliferating T cells (% CFSE-reducing T cells) was higher when co-cultured with H/H-mDCs than N/N-mDCs or N/H-mDCs (Fig. 2d, *upper*). However, there was no significant difference between N/N-mDCs and N/H-mDCs. These results suggest that H-mDCs have higher antigen presentation ability than N-mDCs. Because our data also showed that the expression of HLA-DR in H-imDCs is higher than that in N-imDCs (Table 1), we examined the possibility that H-imDCs may be better able to stimulate allo-T cell proliferation than N-imDCs (Fig. 2d, *lower*). The ability of N/N-imDCs was very weak compared with N/N-mDCs. H/H-imDCs exhibited a similar allo-T cell proliferating ability to N/N-mDCs. Interestingly, the ability of N/H-imDCs was higher than that of N/N-imDCs.

Phagocytosis by DCs differentiated under hypoxia is reduced

Human colonic carcinoma SW640 cells were lysed by five rounds of freeze-thawing to generate necrotic cells. Necrotic SW640 cells were labeled with PKH26 and co-cultured with DCs for 2 h under normoxia or hypoxia, before the percentage (% PKH26-positive cells) of DCs that had captured necrotic SW640 cells and the MFI of PKH-positive necrotic cells captured were measured by FACS analysis (Fig. 3a, b). Both the % PKH26-positive cells and the MFI in H/H-imDCs were remarkably low compared with N/N- or N/H-imDCs (Fig. 3a). These data indicate that H-imDCs contain only small phagocytic populations (Fig. 3a, *middle*) and that the phagocytic ability of these populations is low (Fig. 3a, *right*). However, there was no significant difference between N/N-imDCs and N/H-imDCs. The phagocytic ability of mDCs was remarkably lower than that of imDCs. However, phagocytosis of H/H-mDCs was also lower than that of N/N- and N/H-mDCs (Fig. 3b). When DCs were co-cultured with FITC-dextran for 1 h, the % FITC-positive cells

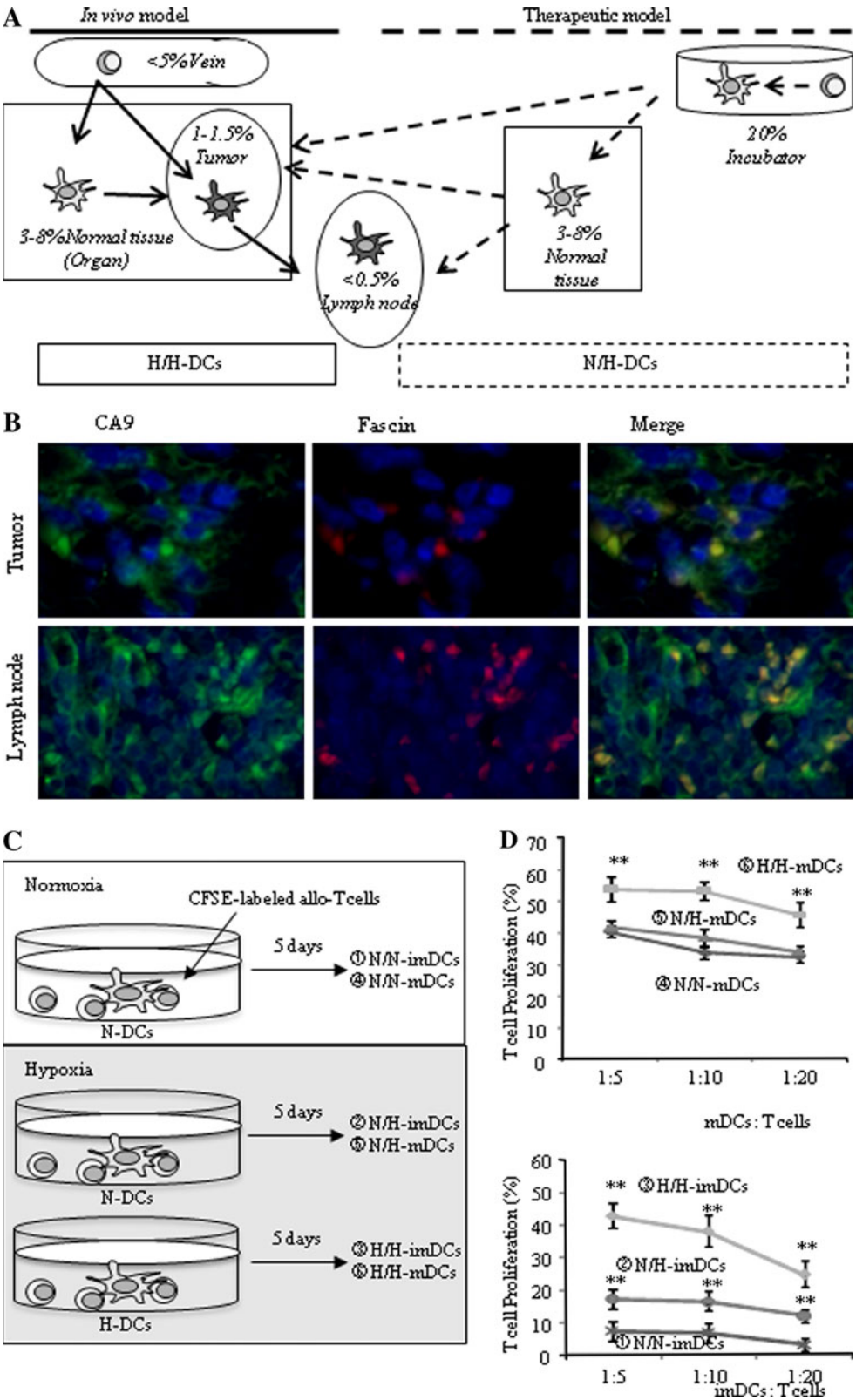

Fig. 2 DCs differentiated under hypoxia exhibit higher allo-T cell proliferating ability. **a** Schematic figure of our model. The in vivo model shows that monocytes differentiate into DCs between 3 and 8% O_2 and DCs then move into tumor tissues of 1–1.5% O_2 (H/H-DCs). The therapeutic model shows that DCs generated from monocytes under 20% O_2 in vitro are injected into subcutaneous tissues of 3–8% O_2 and then move to lymph nodes below 0.5% O_2 (N/H-DCs). b Tumor tissues and regional lymph nodes without metastases were doubly stained with fluoresce-labeled antibodies against with CA9 (*green*; *left picture*) and fascin (*red*; *middle picture*) (× 200). Fascin-expressing DCs also expressed CA9 induced by hypoxia in tumor tissues and lymph nodes (*yellow*; *right picture*) (× 200). **c** Proliferation of allogeneic T cells stimulated by DCs. N-DCs were co-cultured with CFSE-labeled allogeneic T cells for 5 days under normoxia (N/N-DCs) or hypoxia (N/H-DCs). H-DCs were co-cultured under hypoxia (H/H-DCs). **d** DCs were co-cultured with allogeneic T cells at a ratio of 1:5, 1:10, and 1:20 for 5 days under normoxia or hypoxia. The ability of H/H-mDCs to stimulate allogeneic T-cell proliferation was increased (*upper panel*). The ability of N/N-imDCs was very weak compared with N/H- and H/H-imDCs (*lower panel*). Results are expressed as the means ± SD of three independent experiments. $^{**}P < 0.01$ versus N/N-DCs is shown

were similar between H/H-imDCs and N/N-imDCs (Fig. 3c, *middle*). However, the level of phagocytosis of H/H-imDCs was lower than that of N/N-imDCs (Fig. 3c, *right*).

Motility of DCs differentiated under hypoxia is reduced

To capture the antigens, DCs must move to sites where antigen exists. In the present study, cell motility was

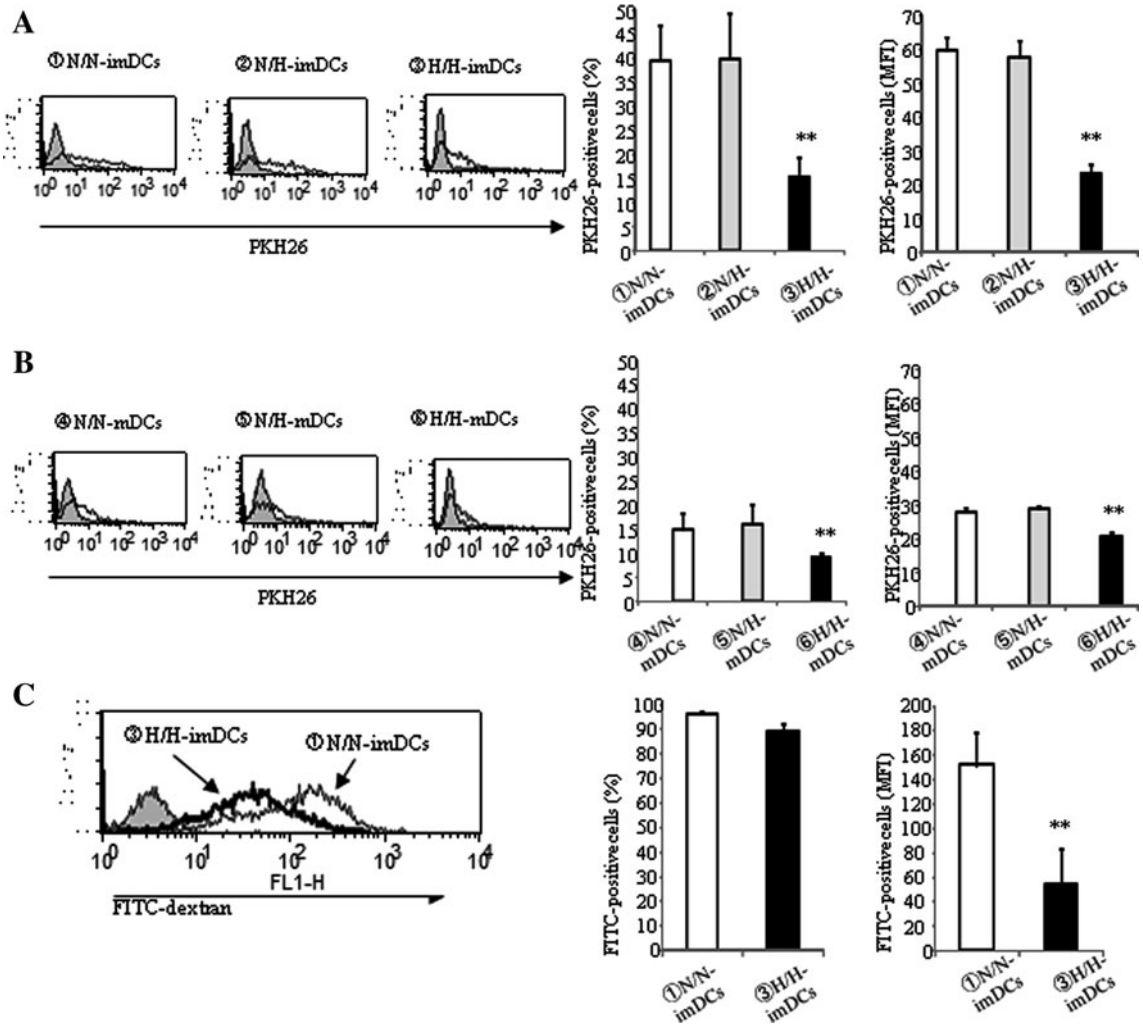

Fig. 3 Phagocytosis by DCs differentiated under hypoxia is reduced. **a**, **b** DCs were cultured with necrotic tissue labeled with PKH26 fluorescence for 2 h at 37°C (*solid line*) or 4°C (*shaded*) under normoxia or hypoxia. The DCs were applied to FACS analysis. Phagocytic ability of H/H-DCs was remarkably low compared with that of N/N-DCs. There was no significant difference between N/N-DCs and N/HDCs. **c** DCs were cultured with opsonized FITC-dextran for 1 h at 37 or 4°C (*shaded*) under normoxia or hypoxia. The quantity of opsonized FITC-dextran uptake by H/H-imDCs was remarkable lower compared with that of N/N-imDCs. *Right panels* the average of three independent experiments is shown. *Bars* show the means plus SD. $^{**}P < 0.01$ versus N/N-DCs is shown

distinguished into random migration (16 h), chemotaxis (3 h), and invasion (16 h). After 16 h, the random migration of H/H-imDCs was decreased by 50% when compared with that of N/N- or N/H-imDCs (Fig. 4a, *upper*), while there was no significant difference between N/N-imDCs and N/H-imDCs. Although the random migration of mDCs was remarkably low compared with imDCs, random migration of H/H-mDCs was also decreased (Fig. 4a, *lower*).

CCR5 expression was found in imDCs but not in mDCs, and the expression intensity was very similar between N/N-, N/H-, and H/H-imDCs (Fig. 4b, *upper left*). On the other hand, CCR7 expression was found in mDCs but not in imDCs except for H/H-imDCs (Fig. 4b, *lower left*). So, we used CCL5 and CCL21 as chemotactic factors for imDCs and mDCs, respectively. The number of migrating H/H-imDCs in response to CCL5 was decreased by 50% when compared with that of N/N- or N/H-imDCs (Fig. 4b, *upper right*). Similarly, migration of H/H-mDCs in response to CCL21 was also decreased by 65% when compared with that of N/N- or N/H-mDCs (Fig. 4b, *lower right*).

The number of invading cells of H/H-imDCs was decreased by 78% when compared with that of N/N- or N/H-imDCs (Fig. 4c, *left*). As we know, the invasive ability of mDCs was remarkably low compared with imDCs. Similarly, however, the number of invading H/H-mDCs was decreased by 73% when compared with N/N- or N/H-mDCs (Fig. 4c, *right*). Since our data suggest that MMP9 is involved in matrigel invasion of DCs (Fig. 1d), we examined *MMP9* mRNA expression in N/H-DCs (data

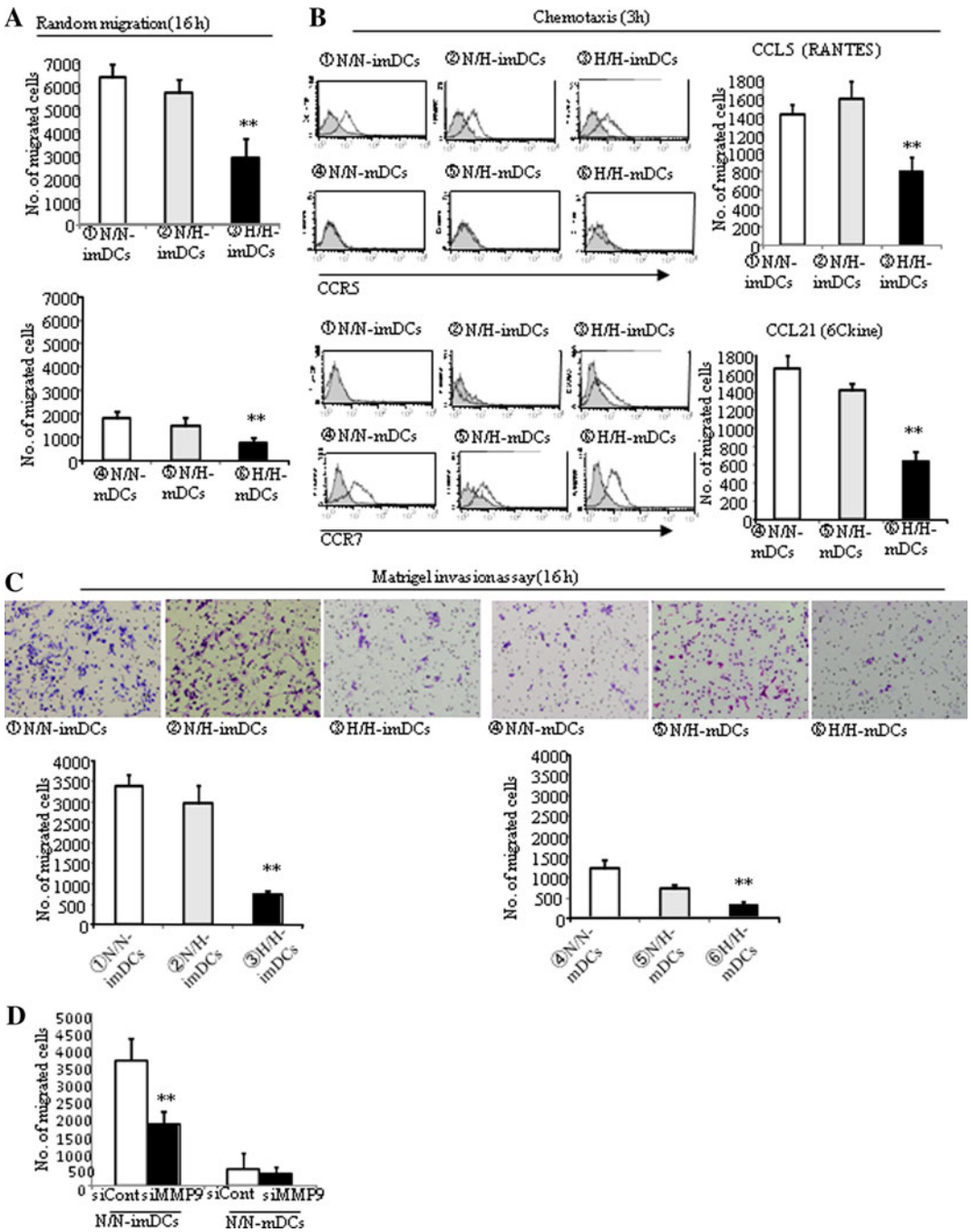

Fig. 4 Motility of DCs differentiated under hypoxia is reduced. **a** Incubation time for the random migration assay was 16 h. The random migration ability of H/H-imDCs was decreased by 50%. The average of three independent experiments is shown. *Bars* show the means plus SD. $^{**}P < 0.01$ versus N/N-DCs is shown. **b** Expression of CCR5 and CCR7 was analyzed by FACS analysis (*left panel*). CCR5 expression was found in imDCs but not in mDCs, and the expression intensity was very similar between N/N-, N/H-, and H/H-imDCs (*upper panel*). CCR7 expression was found in mDCs but not in imDCs except for H/H-imDCs (*lower panel*). Isotype and DCs are presented as *light gray* and *thin black lines* in the histogram. To evaluate the effects of the hypoxia on chemokine receptor function, the chemotactic responsiveness was assessed (*right panel*). The number of migrating H/H-imDCs toward CCL5 was decreased by 50%. Similarly, that of H/H-mDCs toward CCL21 was also decreased by 65%. *Right panels* the average of three independent experiments is shown. *Bars* show the means plus SD. $^{**}P < 0.01$ versus N/N-DCs is shown. **c** DCs that invaded through the Matrigel-coated filter were examined and were counted under a light microscope (× 100) (*upper panel*). The number of invading H/H-imDCs was decreased by 78% (*lower left panel*). The number of invading H/H-mDCs was decreased by 73% when compared with N/N- or N/H-mDCs (*lower right panel*). The average of three independent experiments is shown. *Bars* show the means plus SD. $^{**}P < 0.01$ versus N/N-DCs is shown. **d** The number of invading MMP9-silenced DCs was decreased

not shown). As expected, *MMP9* mRNA expression of H/H-imDCs was remarkably low compared to N/N-imDCs, and that of H/H-imDCs was also lower than that of N/H-imDCs. In addition, the number of invading cells in *MMP9* silencing DCs was also decreased (Fig. 4d), suggesting that matrigel invasion is well correlated with *MMP9* mRNA expression levels.

Inclusive evaluation of complex biological functions of DCs under different oxygen conditions by a 3-D two-layer collagen matrix gel culture system

In order to mimic the in vivo microenvironment of tumor tissues and evaluate inclusively complex in vivo antigen presentation functions of DCs under different oxygen conditions, we used a 3-D two-layer collagen matrix gel culture model we previously developed (Fig. 5a, *upper*) [16]. This model consists of two layers of collagen gels (Fig. 5a, *lower*); the lower contains imDCs labeled with PKH67 (green) and the upper layer contains necrotic tumor cells labeled with PKH26 (red). Using this model, imDCs were cultured for 5 days under normoxia or hypoxia (Fig. 5b). In this system, imDCs that migrated to the upper layer (migrating DCs) and engulfed necrotic cells change from green to yellow (phagocytic DCs). imDCs were collected from collagen gels with collagenase, and the percentage of PKH26-positive imDCs among the total imDCs was estimated as phagocytic ability by FACS analysis. Culture medium was also collected, and the concentration of VEGF and IL-12 was measured.

A lot of N/N-imDCs migrated into the upper layer on day 2 (Fig. 5c *upper*). On the other hand, several N/H-imDCs and only a few H/H-imDCs migrated (Fig. 5c, *middle*, *lower*). On day 5, the % PKH26-positive N/H-imDCs was intermediate between N/N-imDCs and H/H-imDCs (Fig. 5d, *lower left*). The quantity of necrotic cells captured by individual % PKH26-positive N/H-imDCs was also intermediate between N/N-imDCs and H/H-imDCs (Fig. 5d, *lower right*).

Using imDCs collected from collagen gels, the expression of antigen presentation–related molecules was examined by FACS analysis (Table 2). When the upper layer did not contain necrotic cells, expressions of CD80, CD86, HLA-DR, and CD83 in H/H-imDCs were slightly higher than those in N/N-imDCs, indicating a slight maturation during the 5-day culture under hypoxia. In the presence of necrotic cells, most N/N-imDCs often expressed CD80, CD86, HLA-ABC, and HLA-DR, while 30% of cells also expressed CD83. On the other hand, expression of these molecules in H/H-imDCs co-cultured with necrotic cells was similar to that in H/H-imDCs cultured without necrotic cells, excluding the expression of CD86. Data indicate that maturation may require the capture of a suitable quantity of necrotic cells or that imDCs cannot mature merely by capturing necrotic tissues under hypoxia.

Fig. 5 The expression of cytokines, phagocytotic ability, and migration ability in 3-D two-layer collagen gel model under hypoxia was examined. **a**, **b** The *lower layer* contained DCs labeled with PKH67 (*green*), and the *upper layer* contained necrotic cells labeled with PKH26 (*red*). DCs migrated to the *upper layer* and were seen in the same field with necrotic cells. Some of them appeared to be *yellow cells*, implying the phagocytosis of necrotic cells by DCs. **c** Migration of DCs in 3-D two-layer collagen matrix under a light microscope (× 100). A lot of N/N-imDCs migrated toward necrotic cells on day 2. **d** *Upper panel* Migration and phagocytosis of DCs in 3-D two-layer collagen matrix. Fluorescently labeled DCs and necrotic cells were embedded separately into collagen matrix and then observed by fluorescence microscopy (× 100). The number of N/N-imDCs that had engulfed necrotic cells had increased. *Middle*, *lower panel* The DCs were harvested from the collagen matrix and analyzed by FACS analysis on day 5. The % PKH26%-positive N/H-imDCs was intermediate between N/N-imDCs and H/H-imDCs. DCs without necrotic cells and DCs with necrotic cells are presented as light gray and *thin black lines* in the histogram. The average of three independent experiments is shown. *Bars* show the means plus SD. $^{**}P < 0.01$ is shown. **e** IL-12 and VEGF secretion was measured by ELISA in the supernatants collected from 3-D two-layer collagen gel cultures on day 5. IL-12 secretion by H/H-DCs was significantly reduced compared with that by N/N-DCs (*left panel*). In contrast, VEGF secretion was low by N/N-, N/H, and H/H-imDCs (*right panel*). The average of three independent experiments is shown. *Bars* show the means plus SD. $^{**}P < 0.01$ is shown

We know that necrotic cell-capturing DCs spontaneously mature and secrete IL-12 under normoxia [18]. In other words, IL-12 secretion is the final step of the complex in vivo processes of antigen presentation by DCs. In the absence of necrotic cells, imDCs secreted no detectable IL-12 (Fig. 5e, *left*). As expected, N/N-imDCs secreted a large amount of IL-12 in the present of necrotic cells, but IL-12 secretion by H/H-imDCs was significantly lower than that by N/N-imDCs (Fig. 5e, *left*). VEGF secretion was low, and there was no statistical difference between N/N-imDCs and H/H-imDCs (Fig. 5e, *right*).

Up-regulation of MMP2 and down-regulation of VEGF and CD83 by silencing of HIF-1α in DCs

Hypoxia increases HIF-1α in DCs (Fig. 1b). Therefore, we examined whether hypoxia-induced increased HIF-1α plays a role in the antigen presentation abilities of H-DCs. Monocytes were transfected with control siRNA (siCont) or siRNA targeting *HIF-1α* mRNA (siHIF-1). Using these transfected monocytes, imDCs and mDCs were generated under hypoxia (Fig. 6a). Transfection of siRNA targeting *HIF-1α* reduced *HIF-1α* expression by 80% or greater (Fig. 6b). Although H-DCs were smaller in size than N-DCs (Fig. 1c), silencing of *HIF-1α* did not affect the cellular size (Fig. 6c). Concerning the expression of antigen presentation-related molecules, silencing of *HIF-1α*

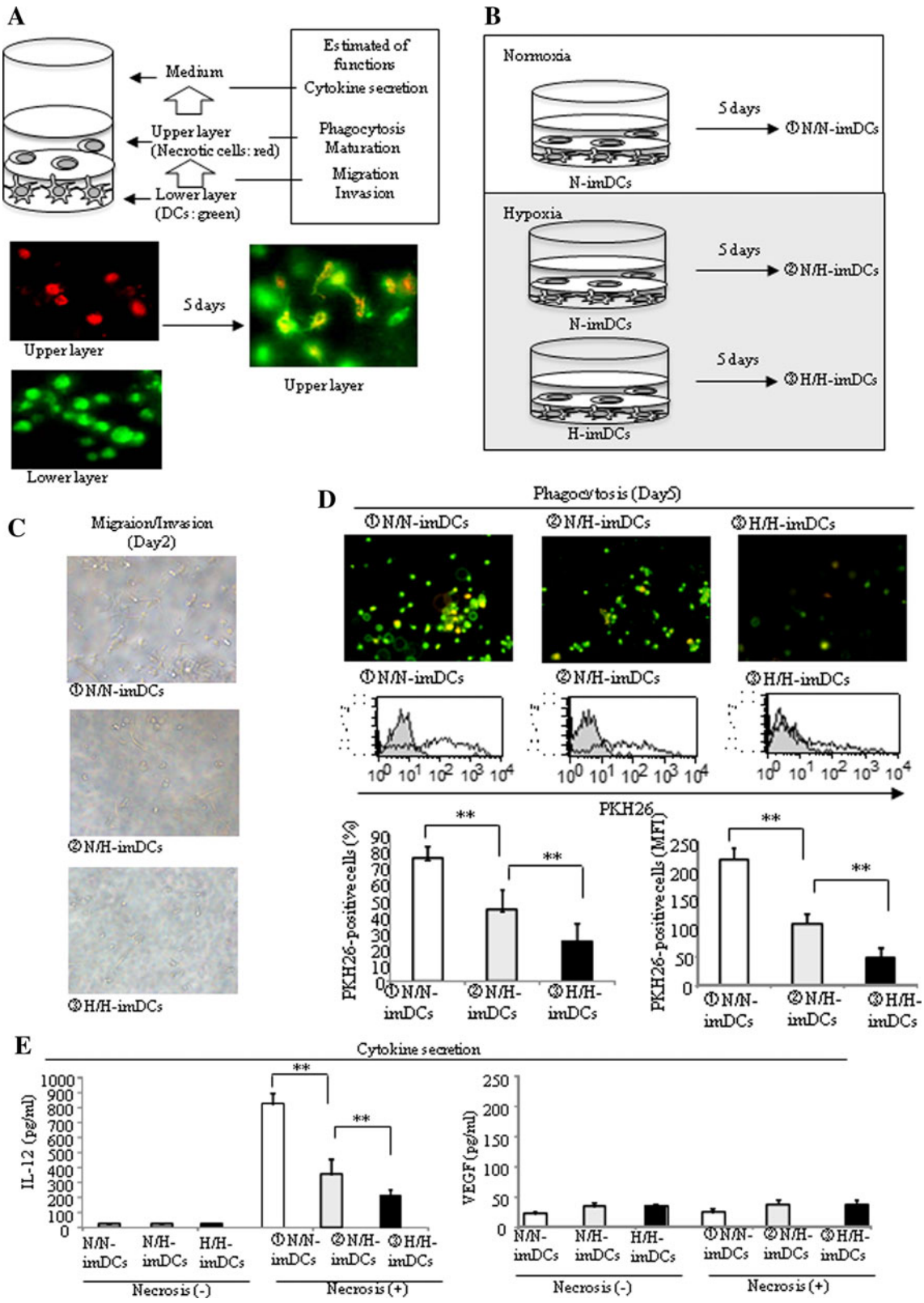

only decreased CD83 expression of H-mDCs (Table 3). In addition, *HIF-1α* silencing reduced the ability of H-mDCs to stimulate allo-T cells (Fig. 6d). *HIF-1α* silencing had little effect on phagocytosis and motility (Fig. 6e–g), only slightly increasing the invasion ability of H-imDCs (Fig. 6h). Interestingly, mRNA expression of *MMP2* but

Table 2 Expression of antigen presentation–related molecules on DCs using 3D-culture system

	Necrotic cells(−) N/N-imDCs	Necrotic cells(−) N/H-imDCs	Necrotic cells(−) H/H-imDCs	①Necrotic cells(+) N/N-imDCs	②Necrotic cells(+) N/H-imDCs	③Necrotic cells(+) H/H-imDCs
CD80	29.99 ± 7.36	28.75 ± 4.37	34.89 ± 10.12	65.53 ± 14.16 *	37.58 ± 8.29	39.17 ± 11.71
	(13.96 ± 4.35)	(15.12 ± 2.69)	(19.72 ± 4.56)	(28.02 ± 2.26)**	(12.92 ± 3.41)	(22.71 ± 2.87)
CD86	31.99 ± 15.1	35.25 ± 13.25	40.45 ± 10.47	75.66 ± 6.87	70.51 ± 3.21	70.92 ± 5.95
	(45.16 ± 26.36)	(50.3 ± 30.87)	(91.33 ± 33.73)	(235.83 ± 79.61)**	(155.17 ± 57.71)	(163.42 ± 31.19)
HLA-ABC	97.97 ± 1.24	98.26 ± 0.78	97.65 ± 1.26	97.69 ± 2.18	98.18 ± 0.84	97.84 ± 1.62
	(147.59 ± 60.77)	(108.01 ± 35.61)	(167.46 ± 53.22)	(291.10 ± 87.83)**	(127.62 ± 41.69)	(185.27 ± 66.52)
HLA-DR	57.22 ± 5.81	62.77 ± 3.29	85.17 ± 13.79	90.24 ± 6.18	92.42 ± 4.42	92.05 ± 5.47
	(44.96 ± 7.76)	(45.32 ± 12.32)	(100.49 ± 21.86)	(135.28 ± 54.23)**	(112.83 ± 31.12)	(118.90 ± 43.59)
CD83	4.52 ± 0.86	3.03 ± 1.3	7.05 ± 3.48	27.44 ± 5.86*	4.24 ± 1.72	7.42 ± 5.92
	(6.61 ± 2.27)	(5.72 ± 1.85)	(6.71 ± 2.78)	(19.59 ± 3.29)**	(10.69 ± 5.57)	(12.98 ± 3.06)

Expression of CD80, CD86, CD83, HLA-ABC, and HLA-DR was analyzed by FACS analysis. DCs were harvested from the collagen matrix and analyzed on day 5

Data are presented as the percentage of positive cells of three independent donors (MFI of each marker)

* $P < 0.05$ (① versus ②, ③: percentage of positive cells)

** $P < 0.05$ (① versus ②, ③: MFI)

not *MMP9* was increased by silencing of *HIF-1α* (Fig. 6i). Finally, we examined the effect of silencing of *HIF-1α* on cytokine production (Fig. 6j). As we expected, silencing of *HIF-1α* markedly decreased VEGF production (Fig. 6j, *right*). On the other hand, IL-12 production was not affected (Fig. 6j, *left*).

Fig. 6 Silencing of HIF-1α in DC regulated MMP2, VEGF, and expression of CD83. **a** Monocytes were transfected with siRNA for HIF-1α for 48 h (siHIF-1). HIF-1α-silenced monocytes were cultured for 5 days with IL-4 and GM-CSF and induced for further maturation by treatment with LPS for 48 h under hypoxia. **b** The expression of HIF-1α was evaluated by real-time RT-PCR and Western blot. Transfection of siRNA targeting HIF-1α reduced HIF-1α expression by 80% or greater. **c** FACS analysis showed that silencing of HIF-1α did not alter the forward and side scatter properties of DCs. **d** H-DCs were co-cultured with allogeneic T cells at a ratio of 1:5, 1:10, and 1:20 for 5 days under hypoxia. HIF-1α silencing reduced the ability of H/H-mDCs to stimulate allo-T cell. Results are expressed as the means ± SD of three independent experiments. *$P < 0.05$ is shown. **e** H-DCs were cultured with necrotic cells labeled with PKH26 for 2 h at 37 or 4°C under hypoxia. FACS analysis showed that silencing of HIF-1α did not affect phagocytosis by H-DCs. **f–h** Only the invasion of H/H-imDCs was slightly increased by silencing of HIF-1α. The average of three independent experiments is shown. *Bars* show the means plus SD. *$P < 0.05$ is shown. **i** mRNA expression was measured by real-time RT-PCR. mRNA expression of MMP2 in HIF-1α silencing DCs was enhanced (*left panel*). Expression of MMP9 mRNA was not affected (*right panel*). **j** IL-12 and VEGF secretion by H-DCs was measured by ELISA

Discussion

In the present study, we focused on two issues. The first was to examine how DCs, which are differentiated from monocytes in vivo and generated from monocytes in vitro, exhibit antigen presentation–related functions under oxygen conditions that mimicked the in vivo microenvironment. Briefly, to estimate the functions of DCs differentiated in vivo under hypoxia, those of H-DCs were examined under hypoxia (H/H-DCs). On the other hand, to estimate the in vivo function of therapeutic DCs generated under normoxia, the functions of N-DCs were examined under hypoxia (N/H-DCs). Then we compared the functions of N/H-DCs and H/H-DCs with those of N-DCs cultured under normoxia (N/N-DCs). The second was to examine simultaneously a series of complex antigen presentation–related functions, consisting of migration, phagocytosis, lymphatic vessel invasion, antigen presentation, and cytokine secretion. In addition, we utilized our 3-D two-layer culture system to estimate inclusively complex in vivo functions [16].

We must first discuss the size of the DCs generated under hypoxia. To our knowledge, this is a novel finding. We have previously reported that DCs generated from cancer patients' monocytes contain a considerable number of dysfunctional small-size populations [19]. The size of H-DCs is similar to that of cancer patients' DCs. However, H-DCs express high levels of antigen presentation–related molecules such as CD80, CD86, and HLA-DR compared to N-DCs, suggesting a high antigen presentation ability of H-DCs. In fact, H/H-mDCs exhibited higher allo-T cell stimulation ability than N/N-mDCs. On the other hand, the ability of N/H-mDCs was similar to that of N/N-mDCs. Taken together, these findings suggest that the T-cell stimulation ability of DCs is dependent upon the oxygen tension at the time when DCs were induced from

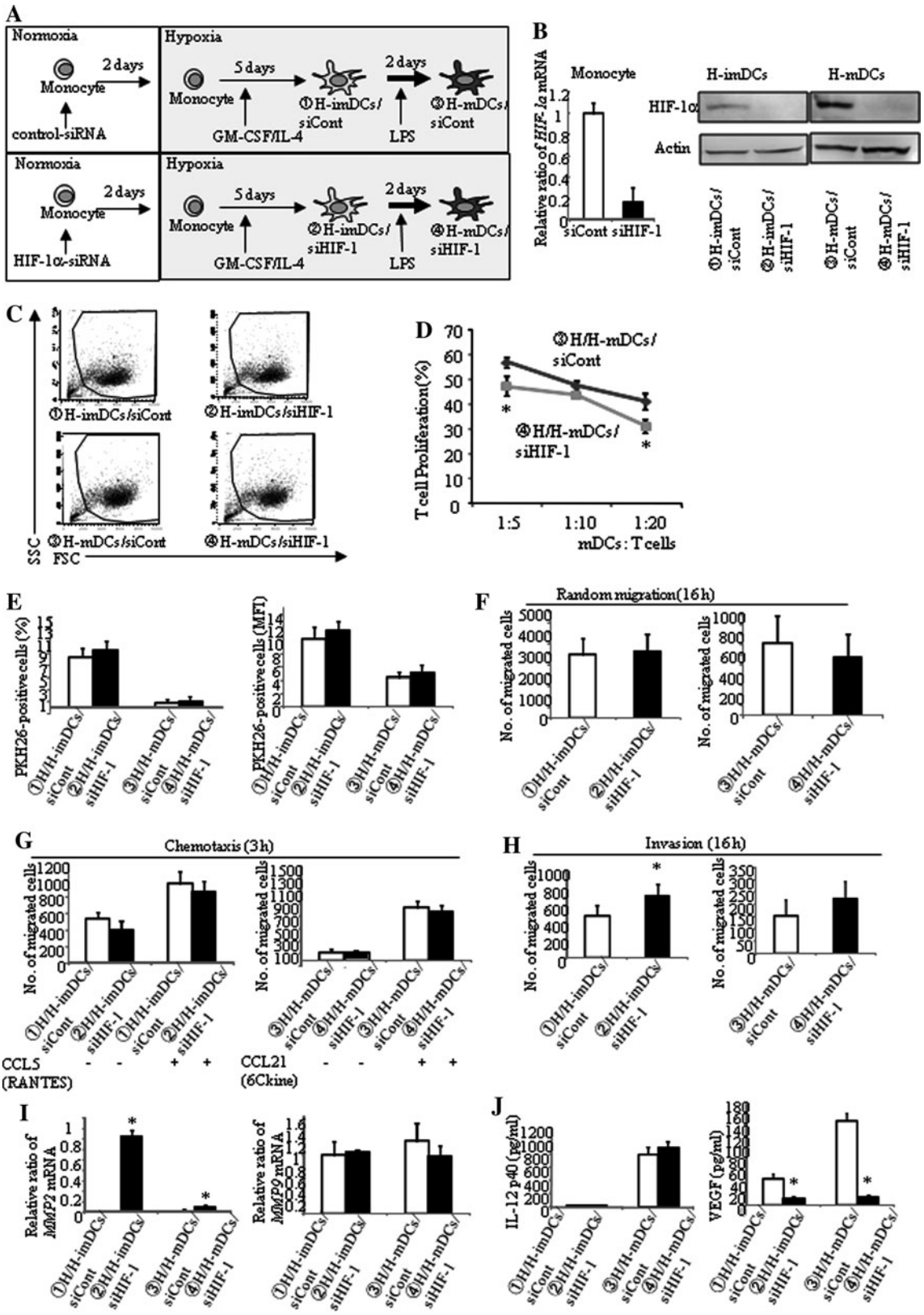
A
Normoxia
Hypoxia
Monocyte
2 days
5 days
2 days
control-siRNA
GM-CSF/IL-4
LPS
①H-imDCs/ siCont
②H-imDCs/ siCont
HIF-1α-siRNA
②H-imDCs/ siHIF-1
④H-mDCs/ siHIF-1
B
Monocyte
H-imDCs
H-mDCs
HIF-1α
Actin
Relative ratio of HIF-1α mRNA
siCont
siHIF-1
C
①H-imDCs/siCont
②H-imDCs/siHIF-1
③H-mDCs/siCont
④H-mDCs/siHIF-1
SSC
FSC
D
③H/H-mDCs/ siCont
④H/H-mDCs/ siHIF-1
T cell Proliferation(%)
1:5
1:10
1:20
mDCs : T cells
E
PKH26-positive cells (%)
PKH26-positive cells (MFI)
F
Random migration(16h)
No. of migrated cells
G
Chemotaxis (3h)
CCL5 (RANTES)
CCL21 (6Ckine)
H
Invasion (16h)
I
Relative ratio of MMP2 mRNA
Relative ratio of MMP9 mRNA
J
IL-12 p40 (pg/ml)
VEGF (pg/ml)

Table 3 Expression of antigen presentation–related molecules on DCs, which were transfected with siRNA targeting *HIF-1α* mRNA

	①H-imDCs/siCont	②H-imDCs/siHIF-1	③H-mDCs/siCont	④H-mDCs/siHIF-1
CD80	31.13 ± 8.05	20.87 ± 10.66	85.90 ± 6.88	79.68 ± 9.46
	(15.69 ± 4.11)	(12.92 ± 4.49)	(92.09 ± 9.72)	(84.75 ± 10.16)
CD86	28.97 ± 9.87	29.34 ± 5.72	96.12 ± 3.11	96.04 ± 3.18
	(74.21 ± 33.15)	(76.64 ± 38.69)	(1,455.77 ± 220.98)	(1,446.16 ± 208.64)
HLA-ABC	98.31 ± 0.18	99.52 ± 0.26	99.12 ± 0.12	99.46 ± 0.18
	(186.61 ± 45.76)	(147.23 ± 42.08)	(609.29 ± 137.09)	(543.40 ± 75.65)
HLA-DR	54.76 ± 10.20	61.94 ± 7.69	92.18 ± 5.60	92.03 ± 2.08
	(42.65 ± 23.25)	(46.89 ± 34.54)	(160.31 ± 20.62)	(160.80 ± 22.79)
CD83	2.58 ± 0.27	1.61 ± 0.15	79.73 ± 15.89	48.61 ± 10.07*
	(5.62 ± 1.59)	(4.02 ± 1.15)	(46.99 ± 9.07)	(33.82 ± 4.41)**

Expression of CD80, CD86, CD83, HLA-ABC, and HLA-DR was analyzed by FACS analysis. Monocytes were transfected with siRNA for *HIF-1α* for 48 h (siHIF-1). *HIF-1α*-silenced monocytes *were* cultured for 5 days with IL-4 and GM-CSF (H-imDCs/siHIF-1) and induced for further maturation by treatment with LPS for 48 h under hypoxia (H-mDCs/siHIF-1). Data are presented as the percentage of positive cells of three independent donors (MFI of each marker), mean ± SD

* $P < 0.05$ (③ versus ④: percentage of positive cells)

** $P < 0.05$ (③ versus ④: MFI)

monocytes rather than the oxygen tension at the time when allo-T cells were stimulated by DCs. On the other hand, the ability of H/H-imDCs was increased to stimulate allogeneic T-cell proliferation. We then examined the effect of DCs on the differentiation of regulatory T cells (Tregs). Strikingly, H/H-imDCs induced higher levels of Tregs compared with N/N-imDCs (data not shown). Thus, there is a possibility that also increased T-cell stimulation by H/H-imDCs may be due to the increased number of Tregs, which we are now investigating. We now guess another possibility that a high density of antigen presentation–related molecules on the small-sized H-DCs may be concerned in this matter.

Consistent with other investigators, our data also revealed the decreased motility and phagocytic ability of H-DCs, with the exception of chemotaxis [13–15, 20–23]. The current study indicated that the decreased invasiveness of H-DCs is mainly due to the decreased transcription of *MMP9* [20, 22, 23]. It has been shown that hypoxia induces the increased invasiveness of pancreatic cancer cells through up-regulation of MMP9 [24], illustrating the quite contrasting effects induced by hypoxia in cancer cells and DCs. On the other hand, it is noteworthy that *HIF-1α* suppressed *MMP2* but not *MMP9* transcription, and silencing of *HIF-1α* slightly increased the invasiveness of H-imDCs. This suggests that MMP2 is partly playing a role in the invasiveness of H-imDCs. It is also profoundly interesting that chemotactic ability is considerably maintained in H-mDCs, because the invasion of mDCs into lymphatic vessels must be strictly regulated [25].

As described above, H-mDCs secreted not only IL-12 but also a considerable amount of VEGF. To our knowledge, there are only a few reports concerning the secretion of VEGF by DCs [26–28]. Our present study demonstrated that H-mDCs produce VEGF through up-regulation of HIF-1α expression. If a similar phenomenon is occurring in vivo, mDCs might secret VEGF in a hypoxic region, such as tumor tissues. We know that VEGF suppresses the functions of DCs [29–31], so the question remains why mDCs secrete VEGF in vivo. We now suggest the possibility that VEGF is working as a negative feedback mechanism to prevent super-activation of mDCs.

It is also a novel finding that HIF-1α may contribute to CD83 expression of H-mDCs. Recently, the possibility is growing that CD83 might be important for DC biology, since it has been shown that the loss of CD83 expression resulted in the impairment of T-cell activation by DCs [32, 33]. During the maturation process, CD83 expression is commonly up-regulated together with CD80 and CD86 [34]. In this present study, however, silencing of *HIF-1α* in H-mDCs reduced CD83 expression without affecting CD80 and CD86 expression. Interestingly, it has been shown that silencing of CD83 by small interfering RNA decreases CD83 expression without influencing the expression of any other molecules and that mDCs not expressing CD83 have dramatically reduced ability to activate T cells [35]. Taken together, mDCs might be carrying out T-cell activation in vivo by increasing the expression of HIF-1α under severe hypoxia.

Finally, we must discuss the data obtained from our 3-D culture system [16]. Using this system, we could grasp inclusively a series of antigen presentation processes performed during a 5-day culture. Differing from in vitro experiments performed under normoxia, data obtained from this culture system indicate that in vivo DCs cannot mature merely by capturing necrotic tumor cells under

hypoxia. Our data also indicate that antigen presentation–related functions of N-DCs are relatively well-maintained compared with H-DCs, when DCs generated for cancer treatment under normoxia were injected subcutaneously or into the tumor site. This is good news for both physicians and patients. However, the bad news is that the apical region of tumors is always exposed to severe hypoxia in pancreatic tissues and that CA9-expressing fascin-positive DCs are often found near the apical region of tumors. That is to say, DCs must break through this hypoxia barrier to infiltrate into the tumor. However, our present data indicate that the invasiveness and phagocytic ability of imDCs that came near the hypoxic area are weakened. Another troublesome affair is that cancer cells existing at apical regions increase their invasiveness and, consequently, efficiently extend the hypoxic areas day by day. In addition, there is the problem that tumors often secrete cytokines, such as TGF-β, which impair the differentiation and function of DCs [36].

Our data suggest that when DCs generated under normoxia is administered in subcutaneous tissue that is under hypoxia, impaired phagocytosis and migration in DCs need to be improved, but we have no idea at this moment. It is reported that VEGF inhibits maturation and function of DCs [29–31]. Anti-VEGF antibody may be useful for improvement of effect in immunotherapy.

In conclusion, we examined a series of antigen presentation processes by DCs under in vivo-mimicking oxygen conditions. We also tried to estimate inclusively these complex functions using our 3-D culture system. Consequently, we could get several different results, which have been reported previously, and new findings concerning the functions of DCs. Most of our data presented here need further investigation, but we believe that it offers valuable information to other investigators.

Acknowledgments We thank Kaori Nomiyama for her skillful technical assistance.

References

1. Galy A, Travis M, Cen D, Chen B (1995) Human T, B, natural killer, and dendritic cells arise from a common bone marrow progenitor cell subset. Immunity 3(4):459–473
2. Randolph GJ, Inaba K, Robbiani DF, Steinman RM, Muller WA (1999) Differentiation of phagocytic monocytes into lymph node dendritic cells in vivo. Immunity 11(6):753–761
3. Caldwell CC, Kojima H, Lukashev D, Sitkovsky MV et al (2001) Differential effects of physiologically relevant hypoxic conditions on T lymphocyte development and effector functions. J Immunol 167(11):6140–6149
4. Hockel S, Schlenger K, Vaupel P, Hockel M (2001) Association between host tissue vascularity and the prognostically relevant tumor vascularity in human cervical cancer. Int J Oncol 19(4): 827–832
5. Sallusto F, Lanzavecchia A (1994) Efficient presentation of soluble antigen by cultured human dendritic cells is maintained by granulocyte/macrophage colony-stimulating factor plus interleukin 4 and downregulated by tumor necrosis factor alpha. J Exp Med 179(4):1109–1118
6. Cella M, Sallusto F, Lanzavecchia A (1997) Origin, maturation and antigen presenting function of dendritic cells. Curr Opin Immunol 9(1):10–16
7. Soruri A, Zwirner J (2005) Dendritic cells: limited potential in immunotherapy. Int J Biochem Cell Biol 37(2):241–245
8. Banchereau J, Steinman RM (1998) Dendritic cells and the control of immunity. Nature 392(6673):245–252
9. Thomas R, Chambers M, Boytar R, Andersen J et al (1999) Immature human monocyte-derived dendritic cells migrate rapidly to draining lymph nodes after intradermal injection for melanoma immunotherapy. Melanoma Res 9(5):474–481
10. Banchereau J, Briere F, Caux C, Palucka K et al (2000) Immunobiology of dendritic cells. Annu Rev Immunol 18:767–811
11. Zinkernagel AS, Johnson RS, Nizet V (2007) Hypoxia inducible factor (HIF) function in innate immunity and infection. J Mol Med 85(12):1339–1346
12. Gale DP, Maxwell PH (2009) The role of HIF in immunity. Int J Biochem Cell Biol 42(4):486–494
13. Mancino A, Schioppa T, Larghi P, Sica A et al (2008) Divergent effects of hypoxia on dendritic cell functions. Blood 112(9): 3723–3734
14. Bosco MC, Pierobon D, Blengio F, Varesio L et al (2009) Hypoxia modulates the gene expression profile of immunoregulatory receptors in human mDCs: identification of TREM-1 as a novel hypoxic marker in vitro and in vivo. Blood 117(9): 2625–2639
15. Bosco MC, Puppo M, Blengio F, Varesio L et al (2008) Monocytes and dendritic cells in a hypoxic environment: spotlights on chemotaxis and migration. Immunobiology 213(9–10):733–749
16. Tasaki A, Yamanaka N, Kubo M, Katano M et al (2004) Three-dimensional two-layer collagen matrix gel culture model for evaluating complex biological functions of monocyte-derived dendritic cells. J Immunol Methods 287(1–2):79–90
17. Kim JB (2005) Three-dimensional tissue culture models in cancer biology. Semin Cancer Biol 15(5):365–377
18. Onishi H, Kuroki H, Katano M, Morisaki T et al (2004) Monocyte-derived dendritic cells that capture dead tumor cells secrete IL-12 and TNF-alpha through IL-12/TNF-alpha/NF-kappaB autocrine loop. Cancer Immunol Immunother 53(12):1093–1100
19. Onishi H, Morisaki T, Kuroki H, Katano M et al (2005) Evaluation of a dysfunctional and short-lived subset of monocyte-derived dendritic cells from cancer patients. Anticancer Res 25(5):3445–3451
20. Qu X, Yang MX, Kong BH, Lu L et al (2005) Hypoxia inhibits the migratory capacity of human monocyte-derived dendritic cells. Immunol Cell Biol 83(6):668–673
21. Ricciardi A, Elia AR, Cappello P, Varesio L et al (2008) Transcriptome of hypoxic immature dendritic cells: modulation of chemokine/receptor expression. Mol Cancer Res 6(2):175–185
22. Zhao W, Darmanin S, Fu Q, Chen J, Kobayashi M et al (2005) Hypoxia suppresses the production of matrix metalloproteinases and the migration of human monocyte-derived dendritic cells. Eur J Immunol 35(12):3468–3477
23. Zhao P, Li XG, Yang M, Qu X et al (2008) Hypoxia suppresses the production of MMP-9 by human monocyte-derived dendritic cells and requires activation of adenosine receptor A2b via cAMP/PKA signaling pathway. Mol Immunol 45(8):2187–2195
24. Du R, Lu KV, Petritsch C, Bergers G et al (2008) HIF1alpha induces the recruitment of bone marrow-derived vascular modulatory cells to regulate tumor angiogenesis and invasion. Cancer Cell 13(3):206–220

25. Faveeuw C, Preece G, Ager A (2001) Transendothelial migration of lymphocytes across high endothelial venules into lymph nodes is affected by metalloproteinases. Blood 98(3):688–695
26. Elia AR, Cappello P, Puppo M, Giovarelli M et al (2008) Human dendritic cells differentiated in hypoxia down-modulate antigen uptake and change their chemokine expression profile. J Leukoc Biol 84(6):1472–1482
27. Nam EH, Park SR, Kim PH (2010) TGF-beta1 induces mouse dendritic cells to express VEGF and its receptor (Flt-1) under hypoxic conditions. Exp Mol Med 42(9):606–613
28. Riboldi E, Musso T, Moroni E, Sozzani S et al (2005) Cutting edge: proangiogenic properties of alternatively activated dendritic cells. J Immunol 175(5):2788–2792
29. Gabrilovich DI, Chen HL, Girgis KR, Carbone DP et al (1996) Production of vascular endothelial growth factor by human tumors inhibits the functional maturation of dendritic cells. Nat Med 2(10):1096–1103
30. Gabrilovich D, Ishida T, Oyama T, Carbone DP et al (1998) Vascular endothelial growth factor inhibits the development of dendritic cells and dramatically affects the differentiation of multiple hematopoietic lineages in vivo. Blood 92(11):4150–4166
31. Alfaro C, Suarez N, Gonzalez A, Perez-Gracia JL et al (2009) Influence of bevacizumab, sunitinib and sorafenib as single agents or in combination on the inhibitory effects of VEGF on human dendritic cell differentiation from monocytes. Br J Cancer 100(7):1111–1119
32. Hirano N, Butler MO, Xia Z, Nadler LM et al (2006) Engagement of CD83 ligand induces prolonged expansion of CD8 + T cells and preferential enrichment for antigen specificity. Blood 107(4):1528–1536
33. Aerts-Toegaert C, Heirman C, Tuyaerts S, Breckpot K et al (2007) CD83 expression on dendritic cells and T cells: correlation with effective immune responses. Eur J Immunol 37(3):686–695
34. Zhou LJ, Tedder TF (1995) Human blood dendritic cells selectively express CD83, a member of the immunoglobulin superfamily. J Immunol 154(8):3821–3835
35. Prechtel AT, Turza NM, Theodoridis AA, Steinkasserer A (2007) CD83 knockdown in monocyte-derived dendritic cells by small interfering RNA leads to a diminished T cell stimulation. J Immunol 178(9):5454–5464
36. Kuga H, Morisaki T, Nakamura K, Katano M et al (2003) Interferon-gamma suppresses transforming growth factor-beta-induced invasion of gastric carcinoma cells through cross-talk of Smad pathway in a three-dimensional culture model. Oncogene 22(49):7838–7847